8828-001

THERMOMECHANICAL TREATMENT OF AN Fe-Mn-Al-C SIDEBAND ALLOY

Kwan H. Han*
Department of Metallurgical Engineering and Materials Science, Carnegie-Mellon University, Pittsburgh, Pennsylvania 15213, USA

*On leave of absence from Yeungnam University, Korea

Tae S. Kang
Department of Metallurgical Engineering, Yeungnam University, 214-1 Daedong, Gyongsan, Kyongbuk, Korea

David E. Laughlin
Department of Metallurgical Engineering and Materials Science, Carnegie-Mellon University, Pittsburgh, Pennsylvania, 15213, USA

ABSTRACT

The influence of thermomechanical treatment on the resulting microstructure and hardening of the Fe-32Mn-8Al-0.9C-0.2Mo sideband alloy has been investigated mainly by means of optical and transmission electron microscopy and microhardness measurements. Two plastic deformation conditions, both giving rise to similar hardness levels, were employed before final aging: one consists of prior deformaiton only and the other is composed of preaging and warm deformation. It is observed that the prior cold deformation renders a significantly higher hardness and that it does not affect the essential mode of continuous precipitation during aging. This treatment, however, causes acceleration of the $\alpha + \beta$-Mn eutectoid reaction, which occurs heterogeneously. This makes the cold deformed alloys extremely brittle. In contrast, in the case of preaged and warm deformed alloys, enhanced hardening, without remarkable acceleration of the heterogeneous eutectoid reaction, is produced during final aging. The warm deformation is observed to cause disturbance in the preaged microstructure, but, apparently, it does not result in any abrupt change of the finally aged microstructure. Preliminary tensile test results indicate that the latter treatment can be effectively used for improving the mechanical properties. The results are compared with those obtained through conventional aging without prior plastic deformation.

THIS WORK has been undertaken to test the applicability of thermomechanical treatment in improving the mechanical properties of age-hardenable Fe-Mn-Al-C austenitic alloys. For this purpose we have examined two different treatments: cold deformation followed by aging and warm deformation during preaging followed by final aging. The effect of each treatment on the hardening response and microstructural change in the Fe-32Mn-8Al-0.9C-0.2Mo alloy has been documented and compared with the conventional aging treatment (no prior plastic deformation).

The potential of age-hardenable Fe-Mn-Al-C alloys for high strength applications has been put forward by several investigators (1-3). These alloys are, however, in effect little more than derivatives of those that were developed earlier (4,5) as a low cost substitute for the traditional Fe-Cr-Ni austenitic stainless steels. The previous investigations (3,6-11) showed that the age hardening in Fe-Mn-Al-C alloys occurs in the course of continuous precipitation of the κ carbide phase ($L'1_2$ type perovskite crystal structure) from the supersaturated austenite matrix. During the initial stage of aging at about 550 °C or below, the parent matrix phase decomposes, exhibiting sidebands in diffraction patterns (6,7,9,11) along with the formation of a modulated structure (3,6-11) consisting of carbon-enriched and carbon-depleted zones alternately aligned in the <100> matrix directions. It has been believed (9) that this decomposition initiates via spinodal decomposition (12). An $L'1_2$ ordering was also observed (3,6-10) to occur in the carbon enriched zones. A recent study (10) showed that the optimum hardening is obtained by the coarsening of this modulated structure. It was also demonstrated (10) that at least about 300 MPa increase of yield strength can be produced, while retaining the total elongation of about 40%, if aging is performed below 550 °C. Previously, an aging experiment using cold deformed alloys was performed by Krivonogov et al. (3). They did not, however, present the microstructural details of their deformed and aged alloys.

EXPERIMENTAL PROCEDURE

The alloy (composition: Fe-31.9 wt.%Mn-8.48 wt.%Al-0.9 wt.%C-0.2 wt.%Mo) (10) was prepared by air induction melting. After homogenization and hot forging at 1200 °C, the alloy was hot rolled at 1150 °C to plates about 3 mm thick.

These plates were then cold rolled without intermediate annealing to 1 mm thick strips. The total amount of cold reduction was 67%. Using these specimens, the following heat treatments were performed:

Treatment I - solution treatment (1027 °C, 600 sec) + 550 °C aging (conventional aging)

Treatment II - 550 °C aging without solution treatment (aging of cold deformed specimens)

Treatment III - solution treatment (1027 °C, 600 sec) + preaging (550 °C, 1.44×10^5 sec) + warm deformation (15% reduction at 550 °C by rolling) + final aging at 550 °C (aging of preaged and warm deformed specimens)

The solution treatment was performed in a vertical type tube furnace under an Ar atmosphere, which was followed by quenching into water. The aging was performed in salt baths consisting of 50%$NaNO_2$-50% KNO_3.

Hardening behavior of specimens with and without prior plastic deformation during final aging was examined mainly by microhardness measurements under a load of 100 g. During the tests, care was taken to make each indentation within an austenite grain. Tensile tests were carried out using specimens with a gauge length of 16 mm and an Instron testing machine. For the tensile tests, the cross-head speed of 3.3×10^{-3} mm/sec (corresponding to an initial strain rate of 2.1×10^{-4}/sec) was used. Microstructural observations were made by optical and transmission electron microscopy (TEM). For optical metallography, specimens were etched in 5% nital solution and thin foils for TEM observations were prepared in a twin-jet electropolisher (9). TEM examination was performed utilizing a Hitachi electron microscope operating at 100 kV.

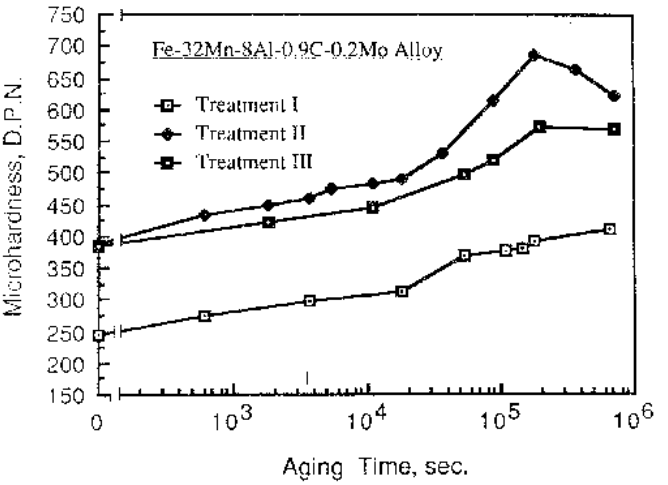

Fig. 1 - 550 °C age hardening curves of specimens with different prior treatments: Treatment I - none, Treatment II - cold deformation, and Treatment III - preaging and warm deformation at 550 °C. (For experimental details, see text.)

RESULTS AND DISCUSSION

Fig. 1 compares the hardening response observed for specimens with and without prior plastic deformation on final aging at 550 °C. Hereafter we will present and discuss the results mainly referring to these aging data.

CONVENTIONAL AGING (TREATMENT I) - The results of this treatment are similar to those reported previously (10). The only difference was in the solution treating condition. In the previous work, the solution treatment was carried out at 980 °C for 1.5×10^3 sec. This slight difference gave rise to a lower hardening in the

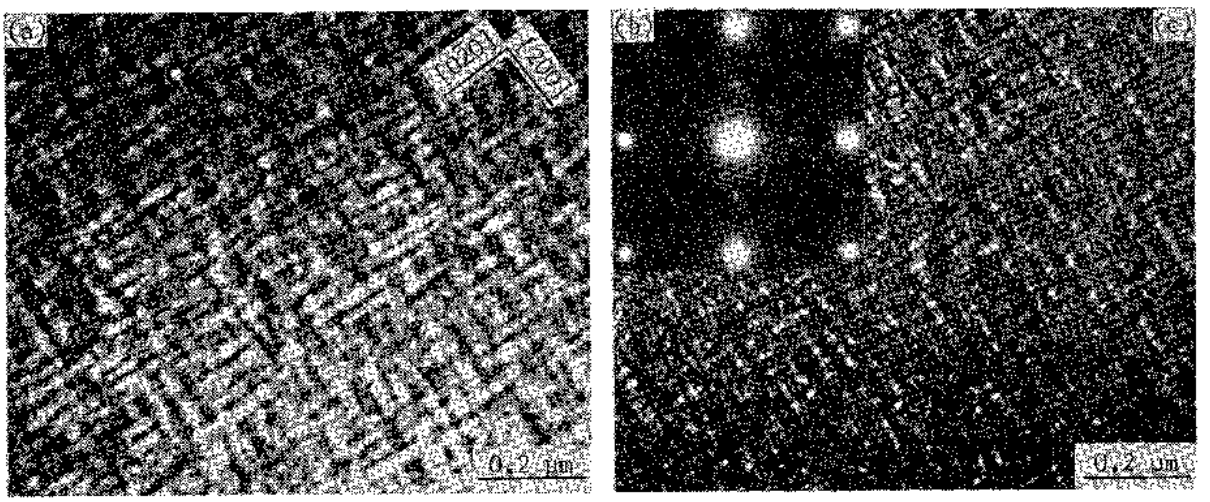

Fig. 2 - TE micrographs of non-deformed specimen after aging for 1.44×10^5 sec at 550 °C: (a) bright field image, (b) corresponding SAD pattern and (c) dark field image taken using 100 superlattice reflection. Foil normal = [002].

present investigation, but the general hardening results were almost same as those in Ref. 10. As seen in Fig. 1, an increase in the hardening rate was observed after the initial moderate hardening. This second stage hardening occurred after aging for 5.4×10^4 sec at 550 °C. Fig. 2 shows both bright and dark field TEM images and the corresponding selected area electron diffraction (SAD) pattern of a specimen aged for 1.44×10^5 sec to produce nearly maximum hardening. In these micrographs, a fairly coarsened {100} two-phase modulated structure can be seen as observed previously (10).

The optical microstructure revealed an apparently austenitic structure, free from grain boundary or heterogeneous precipitation for aging times up to 7.2×10^5 sec. Further prolonged aging, however, produced a cellular like, non-lamellar eutectoid grain boundary reaction, which resulted in the co-precipitation of the β-Mn phase with the ferrite (α) phase (see Fig. 3, for example). This cooperative precipitation corresponds to an α + β-Mn eutectoid reaction, though the term "β-Mn precipitation" frequently appears in the literature (3,6-10) to describe this grain boundary reaction. The β-Mn phase of this eutectoid product is extremely brittle. As a consequence, the occurrence of this eutectoid reaction causes a significant decrease in the ductility (10).

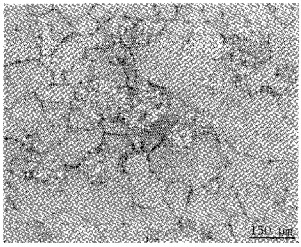

Fig. 3 - Optical micrograph revealing the non-lamellar α + β-Mn eutectoid reaction occurred in non-deformed alloy after aging for 4.3×10^6 sec at 550 °C.

AGING OF COLD DEFORMED SPECIMENS (TREATMENT II) - The cold deformed alloys contained severely distorted austenite grains with many wavy shear bands. TEM examination further revealed many fine bands (transition bands or subgrains (13,14)) with a slight misorientation. The band

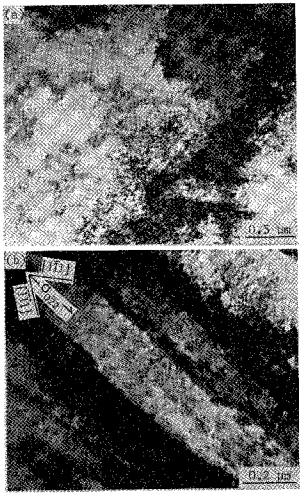

Fig. 4 - Bright field TE micrographs of cold deformed specimens: (a) as-cold deformed, and after aging at 550 °C for (b) 9.4×10^4 sec and (c) 3.6×10^5 sec, respectively. Foil normals; (b) [022] and (c) [002].

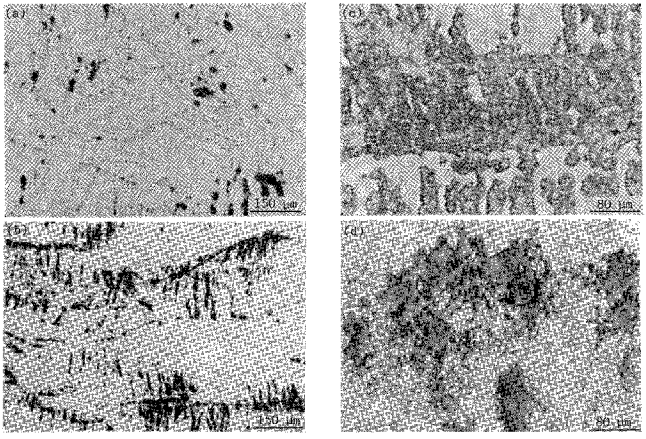

Fig. 5 - Optical micrographs of cold deformed specimens after aging at 550 °C for (a) 5.4×10^3 sec, (b) 1.1×10^4 sec, (c) 3.6×10^3 sec, and (d) 7.2×10^3 sec, respectively. Note the occurrence of the non-lamellar eutectoid reaction along the shear bands as well as at the grain boundaries.

spacing was about 0.1 μm. Fig. 4-a, taken from an as-cold deformed specimen, shows high density of inhomogeneously distributed, tangled dislocations as well as subgrains. Aging of these cold deformed specimens produced a considerably higher hardness. However, in spite of the high density of dislocations and other defects generated during the heavy deformation, the initial rate of hardening was observed to be approximately the same at this aging temperature compared to that for the non-deformed specimens (see Fig. 1). Significantly enhanced hardening (second stage) in the cold deformed specimens occurred after aging for about 3.6×10^4 sec.

To investigate the microstructural change responsible for this hardening TEM examination was performed. It was, however, difficult to observe the decomposed microstructure because of the high degree of deformation and the resulting large number of dislocations. Only weak superlattice reflections could be observed for aging times up to 9.4×10^4 sec (see the corresponding microstructure in Fig. 4-b). Longer aging allowed some recovery to occur, and this enabled the observation of the underlying two-phase modulated microstructure (see Fig. 4-c). This shows that the continuous decomposition mode of spinodal decomposition in this Fe-Mn-Al-C alloy was not substantially affected by the presence of high density of lattice defects (mainly dislocations) introduced by severe prior cold deforamtion. This result is also consistent with previous observations for other cold deformed spinodal alloys such as Cu-Ni-Sn (15,16), Cu-Ti (14,17), Co-Ti-X (18) and Fe-Mo based alloys (19).

The rate of increase of microhardness is seen to be approximately the same for Treatments I and II (Fig. 1). This might be interpreted to indicate that the age hardening mechanism in both is essentially the same in that the hardening occurs with the development of the modulated structure. As shown before, this decomposition process is nearly independent of the lattice defects in the initial microstructure because it occurs via the homogeneous spinodal process (9). However, after aging for about 3×10^4 sec, the hardening in the cold deformed alloy was greater than that in conventionally aged alloy as seen in Fig. 1.

Unfortunately, however, the prior cold deformation was observed to greately accelerate the $\alpha + \beta$-Mn cutectoid reaction. This can be seen in Fig. 5. It is noted in these optical micrographs that the eutectoid reaction occurred even at the shear bands, where slip localization had taken place. Hence, the fast eutectoid reaction rate as seen in Fig. 5 can be due to the

increase of favorable nucleation sites as well as enhanced diffusion owing to high density of lattice defects. Because of this fast rate of the $\alpha + \beta$-Mn reaction, the cold deformed alloy became extremely brittle. For this reason, it is concluded that this treatment of prior cold deformation is not desirable to obtain high strength in Fe-Mn-Al-C alloys.

AGING OF PREAGED AND WARM DEFORMED SPECIMENS (TREATMENT III) - This process was intended to find an alternative method to attain an improvement in hardening by effectively suppressing the acceleration of the $\alpha + \beta$-Mn eutectoid reaction, which occurred when we introduced plastic deformation (Treatment II). To do this we employed preaging and warm deformation treatments. The preaging condition was selected to be near the maximum hardening condition of the conventional aging (Treatment I), which produced a coarsened two-phase modulated structure as seen in Fig. 2. The warm deformation of 15% in reduction was applied to the preaged specimens, thereby making them possess nearly the same level of microhardness as that of as-cold deformed specimen of Treatment II.

In the warm deformed state, the dislocation tangles and subgrains, observed in the cold deformed alloy (Treatment II), were not observed. In addition, thin deformation twins, reported (8) in optimally aged and cold deformed (25% in reduction) Fe-Mn-Al-C alloys, were not observed either. However, the uniformity of the modulated structure of the preaged microstructure was observed to be disrupted as shown in Fig. 6-a. This disruption is obviously due to the repeated movements of dislocations during the warm deformation, which shear the modulated structure. Nevertheless, the modulation wavelength was apparently unchanged (about 27 nm). It is likely, however, that some change in the amplitude of the fluctuations have occurred during deformation as observed in fatigued Cu-Ni-Sn spinodal alloys (20).

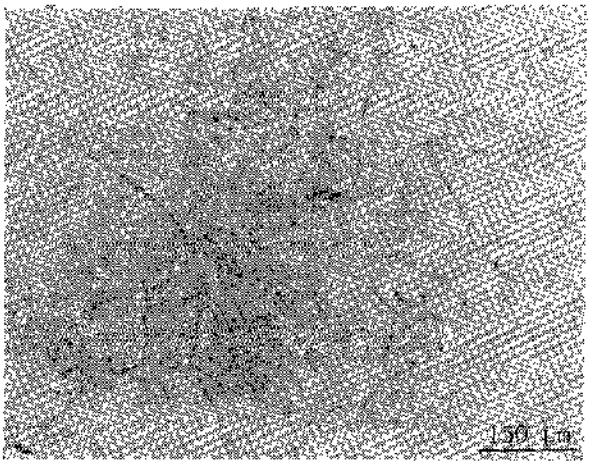

Fig. 7 - Optical micrograph of preaged and warm deformed alloy after final aging for 1.94×10^5 sec at 550 °C.

As seen in Fig. 1, a considerable hardening was further attained by the final aging treatment of the warm deformed alloys. In particular, it is interesting to note that, although the warm deformed alloys have experienced the preaging to produce near maximum hardening in the non-deformed state, further age hardening occurred with a rate almost the same as that of non-deformed alloys. In Fig. 6-b, the TEM microstructure of the warm deformed specimen after aging for 9.4×10^4 sec is shown. It is seen that this aged microstructure looks more like that of non-deformed alloy (Fig. 2) than that of the as-warm deformed alloy (Fig. 6-a). That is, the modulations are more uniform; in effect the microstructure has recovered without remarkable coarsening.

Of importance in this thermomechanical treatment is that the improvement of hardening could be obtained successfully without inducing accel-

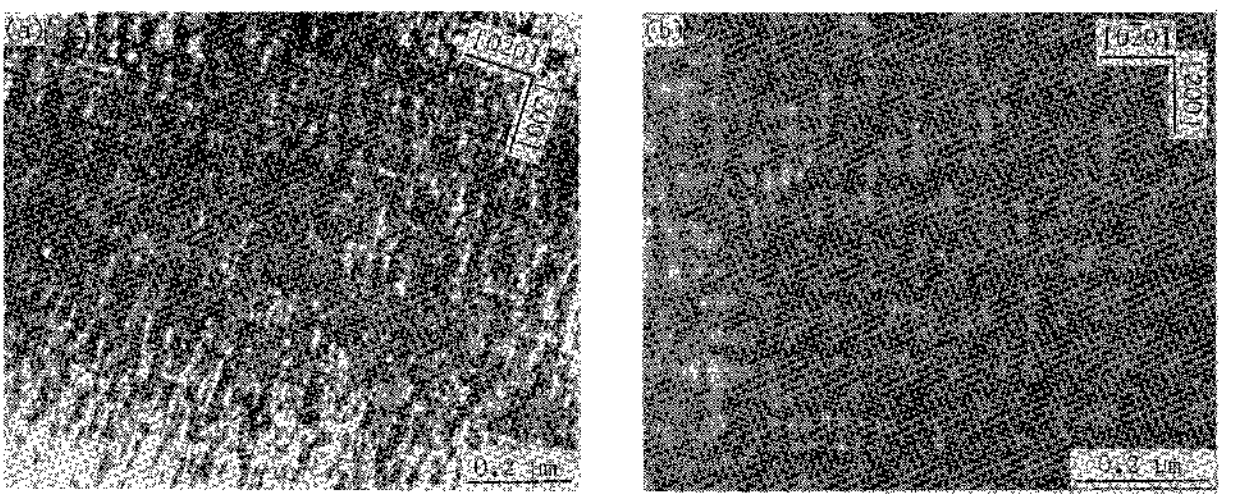

Fig. 6 - Bright field TE micrographs of preaged and warm deformed specimens: (a) as-warm deformed and (b) after aging for 9.4×10^4 sec. Foil normals = [002].

Table 1 Comparision of room temperature tensile properties of non-deformed (Treatment I) and preaged and warm deformed (Treatment III) specimens after aging at 550 °C

Heat treating condition	0.2% yield stress (MPa)	Ultimate tensile stress (MPa)	Elongation (%)
As-solution treated*	373	801	52
Non-deformed after aging for 1.44×10^5 sec*	666	1035	38
Preaged and warm deformed after aging for 1.94×10^4 sec	898	1135	30

* Tensile data of these specimens are somewhat different from those of previous work (10). This may be due to difference in the solution treating condition and tensile test condition.

eration of the $\alpha + \beta$-Mn eutectoid reaction. Fig. 7 shows the optical microstructure of the warm deformed specimen after aging for 1.94×10^5 sec, which produced the maximum hardness. The absence of the grain boundary (eutectoid) reaction can be noted in this micrograph.

The above results obtained through introducing the preaging and warm deformation before final aging implies that this kind of thermomechanical treatment can be effectively used for improving the mechanical properties of Fe-Mn-Al-C sideband alloys. To evaluate this implication we performed preliminary tensile tests. The test results are given in Table 1. It is noted that, as expected from the microhardness and optical metallography results, a considerable increase of yield strength was achieved without significant sacrifice in elongation: the 0.2% yield stress increment was as high as about 260 MPa, compared to that of non-deformed specimen, and this yield stress was about 2.4 times higher than that of as-solution treated specimen.

To optimize the process parameters in the development of mechanical properties and to obtain a better understanding of structure/property relationships of the preaged and warm deformed alloys further work will be undertaken.

SUMMARY

Two thermomechanical treatments were examined to test their applicability in improving the mechanical properties of Fe-Mn-Al-C sideband alloys. For this purpose, the influence of these treatments on the microhardness and the resulting microstructure was investigated using the Fe-32Mn-8Al-0.9C-0.2Mo alloy. It was observed that prior cold deformation produces a significantly higher hardness during the subsequent aging and that it does not alter the essential mode of continuous precipitation. This treatment, however, did induce the acceleration of the undesirable $\alpha + \beta$-Mn eutectoid reaction, thereby making the cold deformed alloys extremely brittle after aging. On the other hand, by utilizing preaging and warm deformation before final aging, enhanced hardening could successfully be attained by suppressing the acceleration of the eutectoid reaction. Preliminary tensile tests showed that, by employing preaging and warm deformation, a high yield strength increase could be attained without significant sacrifice in elongation. The present results suggested that the thermomechanical treatment composed of preaging, warm deformation and final aging can be effectively used for improving the mechanical properties of the Fe-Mn-Al-C sideband alloys.

ACKNOWLEDGMENT

The financial support of the Korea Science and Engineering Foundation (KHH) and the National Science Foundation, DMR-84-13115 at Carnegie-Mellon University (DEL) is gratefully acknowledged.

REFERENCES

1. R.E. Cairns and J.L. Ham, U.S. Patent no. 3,111,405
2. G.L. Kayak, Met. Sci. Heat Treat., (2), 95-97 (1969)
3. G.S. Krivonogov, M.F. Alekseyenko and G.G. Solov'yeva, Phys. Met. Metall., 39, 86-92 (1975)
4. J.L. Ham and R.E. Cairns, Product Eng., 29, 50-52 (1958)
5. D.J. Schmatz, Trans. ASM, 52, 898-913 (1960)
6. N.J. Storchak and A.G. Drachinskaya, Phys. Met. Metall., 44, 123-130 (1977)
7. K.H. Han and W.K. Choo, Metall. Trans. A, 14A, 973-975 (1983)
8. I.S. Kalashnikov, V.S. Litvinov, M.S. Khadyyev and L.D. Chumakova, Phys. Met. Metall., 57, 160-164 (1984)
9. K.H. Han, J.C. Yoon and W.K. Choo, Scripta Metall., 20 (1986)
10. K.H. Han, W.K. Choo, D.Y. Choi and S.P. Hong, Proceedings of Alternate Alloying for Environmental Resistance, G.R. Smolik and S.K. Banerji Eds., 91-106 (1987)
11. K.H. Han and W.K. Choo, unpublished research
12. J.W. Cahn, Trans. AIME, 242, 166-180 (1968)
13. R.D. Doherty, Metal Sci., 8, 132-142 (1974)

14.J. Dutkiewicz, Metall. Trans. A, 8A, 751-761 (1977)
15.J.T. Plews, Metall. Trans. A, 6A, 537-544 (1975)
16.S. Spooner and B.G. Lefevre, Metall. Trans. A, 11A, 1085-1093 (1980)
17.J. Dutkiewicz, Met. Technol., 5, 333-340 (1978)
18.J. Singh, J. Mater. Sci., 21, 1134-1138 (1986)
19.M. Doi, H. Tanabe and T. Miyazaki, J. Mater. Sci., 22, 1328-1334 (1987)
20.M.P. Quin and L.H. Schwartz, Mater. Sci. Eng., 46 (1980)